Progress In Electromagnetics Research C, Vol. 77, 175–184, 2017

Low-Profile Dual-Band Superstrate Antenna Using Metasurface

Jae-Gon Lee[1] and Jeong-Hae Lee[2, *]

Abstract—A low-profile superstrate antenna operated at dual-band is proposed using a metasurface (MTS). In order to design the proposed antenna, the MTS as a partially reflective surface (PRS) has a zero degree reflection phase at dual-band and is composed of a substrate, periodic metallic square patches, and rings on one side and periodic metallic meshes on the other side. To satisfy the resonance condition of Fabry-Perot cavity (FPC) at a certain frequency and height of PRS from the ground plane, the reflection phase of the MTS should be controlled by the dimension of the substrate, square patch, square ring, and mesh. In this paper, the planar radiator having a ring patch and a rectangular patch is employed and designed to operate at 2.1 GHz and 5.8 GHz. Also, the height of MTS from the ground plane is 12 mm, which corresponds to about $0.08\lambda_0$ and $0.23\lambda_0$ at operation frequencies of radiator, respectively. As a result, the gain improvements at 2.1 GHz and 5.8 GHz are measured to be 4.1 dB and 3.2 dB, respectively.

1. INTRODUCTION

Generally, patch antennas are attractive and popular due to characteristics of low-profile, simple structure, and low cost of fabrication. However, one of the major disadvantages usually associated with a patch antenna is a low gain. There have been many studies for the gain improvement of a patch antenna. The conventional solution is to use an array of antennas. However, we might face difficulties such as a complex feed network and degradation of the antenna performance by coupling between elements. Another powerful solution is a combination of antenna and superstrate similar to a Fabry-Perot cavity (FPC) antenna. The partially reflective surface (PRS) as a superstrate has been proposed to increase the gain of the antenna [1]. The principle of the paper based on multiple reflections is described using a ray theory approach. For decades, the superstrate of either high permittivity or permeability has been analyzed using a transverse equivalent network (TEN) model when the source is a horizontal electric Hertzian dipole [2, 3]. Then, a low-profile, high gain antenna using an artificial magnetic conductor (AMC) [4] and metasurface (MTS) [5] has been proposed [6–9]. The height of the high gain superstrate antenna can be determined by the sum of reflection phases of the ground plane and the PRS. Under this condition of height and the reflection phases, the transmitted rays are in-phase, resulting in the improvement of gain. In [7], the AMC ground plane can have a reflection phase from 180 to −180 degrees unlike a PEC ground plane, so that a low-profile superstrate antenna can be designed by the combination of the AMC ground plane and PRS composed of a dielectric and patches. The utilized AMC structure, composed of patches and grounded vias, is operated at single-band, so that it is impossible to design a low-profile superstrate antenna having the height (d) satisfying the resonance condition at an adjacent dual-band. Similarly, a low-profile superstrate antenna can also be designed by the combination of AMC ground plane and MTS having a reflection phase from 180 to −180 degrees [8]. This kind of low-profile superstrate antenna can be designed with an adjacent dual-band but has the

Received 6 June 2017, Accepted 29 August 2017, Scheduled 6 September 2017

* Corresponding author: Jeong-Hae Lee (jeonglee@hongik.ac.kr).

[1] Metamaterial Electronic Device Research Center, Hongik University, Seoul 04066, Korea. [2] School of Electronic and Electrical Engineering, Hongik University, Seoul 04066, Korea.

disadvantage of controling the phase of two artificial surfaces simultaneously to satisfy the resonance condition at dual-band.

In this paper, a low-profile superstrate antenna operated at an adjacent dual-band is proposed and designed using a dual-band MTS and PEC ground plane. Since we only have to control the phase of one artificial MTS, it is easy to design in dual-band. The dual-band MTS consists of a substrate, periodic square patches and rings on one side, and periodic meshes on the other side to achieve zero reflection phase in dual-band. In addition, the radiator operated as a source is designed using a rectangular patch and a ring patch to work in dual-band. In Section 2, we investigate the characteristics of the proposed dual-band MTS and introduce how to control the phases in dual-band. Thus, it is possible to design a low-profile superstrate antenna operated in dual-band and having a certain height. In Section 3, after designing the source antenna operated in dual-band, the performances of the proposed antenna such as reflection coefficient and far-field radiation patterns are simulated and measured.

2. DESIGN OF DUAL-BAND METASURFACE

Figure 1 shows a resonant cavity formed by a PEC ground and a partially reflective surface (PRS) with excitation inside a cavity. When the source is located inside a cavity, as shown in Fig. 1, the directivity of a cavity antenna is given by [1]

$$D = \frac{1 - \Gamma_{PRS}^2}{1 + \Gamma_{PRS}^2 - 2\Gamma_{PRS}\cos\left(\phi_{PRS} + \phi_{GND} - \frac{4\pi}{\lambda}d\right)} f^2 \tag{1}$$

where Γ_{PRS} is the reflection magnitude of the PRS, ϕ_{PRS} the reflection phase of the PRS, ϕ_{GND} the reflection phase of the ground plane, d the height of PRS from ground plane, and f the radiation pattern of the source. To obtain maximum directivity, $\phi_{PRS} + \phi_{GND} - \frac{4\pi}{\lambda}d$ at denominator and the reflection magnitude of the PRS should be 0 and close to 1, respectively. Then, the resonance condition becomes

$$d = (\phi_{PRS} + \phi_{GND})\frac{\lambda}{4\pi} + N\frac{\lambda}{2}, \quad (N = 0, 1, 2, \ldots). \tag{2}$$

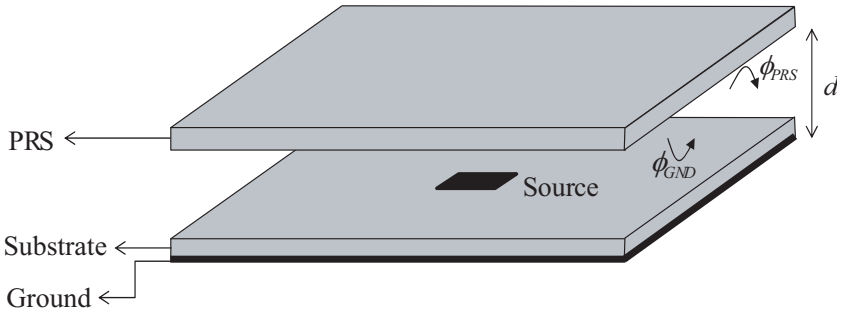

Figure 1. Resonant cavity by PEC and PRS with excitation inside a cavity.

For instance, if the PRS is implemented by a dielectric, and a ground of the antenna is a PEC, the height (d) becomes half wavelength [1].

In this paper, to design the low-profile superstrate antenna operated at dual-band, a metasurface (MTS) having a zero degree reflection phase at dual-band is adopted as a PRS. Figs. 2(a) and 2(b) depict a unit cell of MTS at one side and the other side, respectively. The MTS is composed of a substrate, periodic square patches and rings, and periodic meshes. The equivalent transmission line model of the dual-band MTS is shown in Fig. 2(c). C_1 and L_1 are generated by the square patch and the mesh, respectively. In addition, C_2 and L_2 are generated by the square ring. To show the effects of the component values in the equivalent transmission line in Fig. 2(c), we calculate the reflection coefficients using the equivalent transmission line for the MTS against various component values, as shown in Fig. 3. As a distance between the square patch and ring gets closer, the value of C_1 increases, and the first resonance frequency moves toward the lower frequency. When the width of the mesh

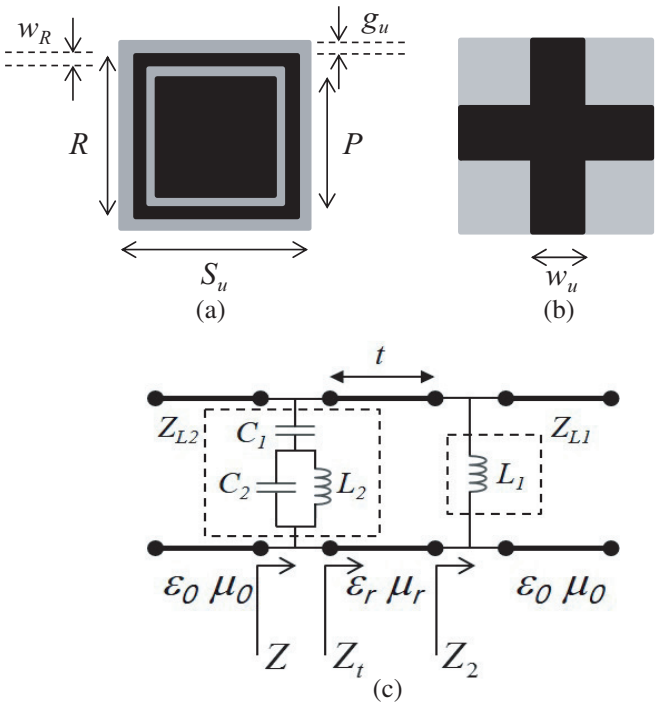

Figure 2. Unit cell of MTS. (a) One side. (b) The other side. (c) Its equivalent transmission line model.

becomes smaller, and the value of L_1 increases, the first resonance frequency is down-shifted. Moreover, the second resonance frequency is inversely proportional to C_2 and L_2. It is noted that the first and second resonance frequencies can be independently controlled by the circuit components of C_1 and L_1, and C_2 and L_2, respectively. The designed dual-band MTS is operated as a band-pass filter (BPF) by C_1/L_1 and C_2/L_2, and has a reflection phase of 0 degree at resonance frequency of BPF. The analytic reflection phase can be calculated by Equation (3).

$$Z_{L1} = j\omega L_1, \quad Z_{L2} = \frac{j\omega C_1 + j\omega C_2 + \dfrac{1}{j\omega L_2}}{j\omega C_1\left(j\omega C_2 + \dfrac{1}{j\omega L_2}\right)} \tag{3a}$$

$$Z_2 = \frac{Z_{L1}Z_0}{Z_{L1}+Z_0}, \quad Z_t = Z_r\frac{Z_2 + jZ_r\tan\beta_r t}{Z_r + jZ_2\tan\beta_r t} \tag{3b}$$

$$Z = \frac{Z_{L2}Z_t}{Z_{L2}+Z_t}, \quad \Gamma = \frac{Z - Z_0}{Z + Z_0} \tag{3c}$$

where Z_0 and Z_r are $\sqrt{\mu_0/\varepsilon_0}$ and $\sqrt{\mu_r\mu_0/\varepsilon_r\varepsilon_0}$, respectively. The values of components in Fig. 2(c) are extracted and optimized from the simulated results of a two-port network for calculation of the analytic reflection phase ($C_1 = 1.2\,\text{pF}$, $L_1 = 2.5\,\text{nH}$, $C_2 = 1.3\,\text{pF}$, and $L_2 = 0.6\,\text{nH}$). Also, to calculate the full-wave simulated reflection phase using Ansys HFSS, we utilize master/slave boundary and Floquet port for an infinite periodic structure and incidence of plane wave, respectively. The design parameters are as follows: $S_u = 8.5\,\text{mm}$, $R = 8.3\,\text{mm}$, $P = 6.5\,\text{mm}$, $w_R = 0.7\,\text{mm}$, $g_u = 0.1\,\text{mm}$, $w_u = 1.5\,\text{mm}$, dimension of patch for single-band = 8.3 mm by 8.3 mm.

Figure 4 shows the analytic and simulated reflection coefficients of the proposed dual-band MTS. The simulated results are in good agreement with the analytic ones. We have fabricated the MTS, which has a dimension of 144.5 mm × 144.5 mm, and the number of unit cells of 17 × 17, as shown in Fig. 5. The periodic patches and meshes are printed on a dielectric slab of thickness 1.6 mm and $\varepsilon_r = 10.2$. After adding the metallic ring structure, we can obtain the MTS with reflection phase of 0 degree at

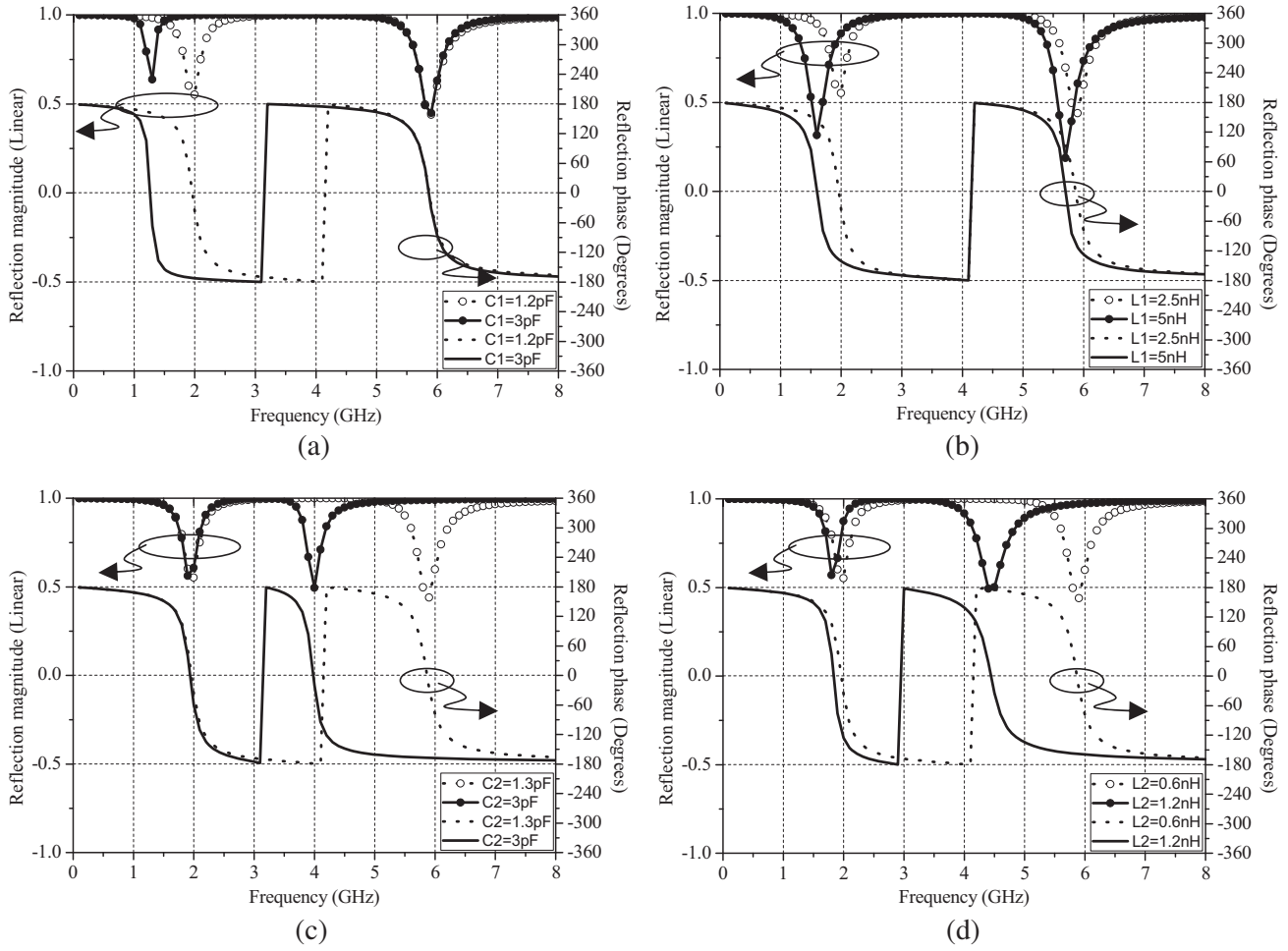

Figure 3. Parametric studies of reflection coefficients for the MTS against various component values in the equivalent transmission line. (a) C_1. (b) L_1. (c) C_2. (d) L_2.

dual-band. The analytic, full-wave simulated, and measured reflection phases of the MTS with periodic patches and meshes (Single-band), and periodic patches/rings and meshes (dual-band) are compared in Fig. 6. The MTS with reflection phase of 0 degree is simulated and measured at 1.9 GHz/5.8 GHz and 2 GHz/5.85 GHz, respectively. The measured results are in good agreement with the analytic and simulated ones. The slight difference between simulated and measured data is caused by manufacturing accuracy and material tolerance. When a PEC ground plane is used for design of the radiator, height (d) of MTS from the ground plane can be calculated using Equation (2).

Figure 7 compares the height of superstrate of single-band MTS (patch and mesh) and dual-band MTS (patch/ring and mesh) satisfying the resonance condition. Even though the single-band MTS can operate at multi-band using harmonic modes ($N = 1, 2, 3 \ldots$) of Equation (2), it is impossible to design a low-profile superstrate antenna having height (d) satisfying the resonance condition at an adjacent dual-band as shown in Fig. 7. If the operation frequencies of source radiator are 2.1 GHz and 5.8 GHz, the height (d) must be equal to 12 mm from measured reflection phase of dual-band MTS. The height of 12 mm corresponds to $0.08\lambda_0$ and $0.23\lambda_0$ at operation frequencies of the radiator, respectively.

3. DUAL-BAND LOW-PROFILE SUPERSTRATE ANTENNA

To design a corresponding dual-band source, a planar patch antenna, which is composed of a rectangular patch for a high band, a ring patch for a low band, and a gap feed, is discussed as a source, as shown

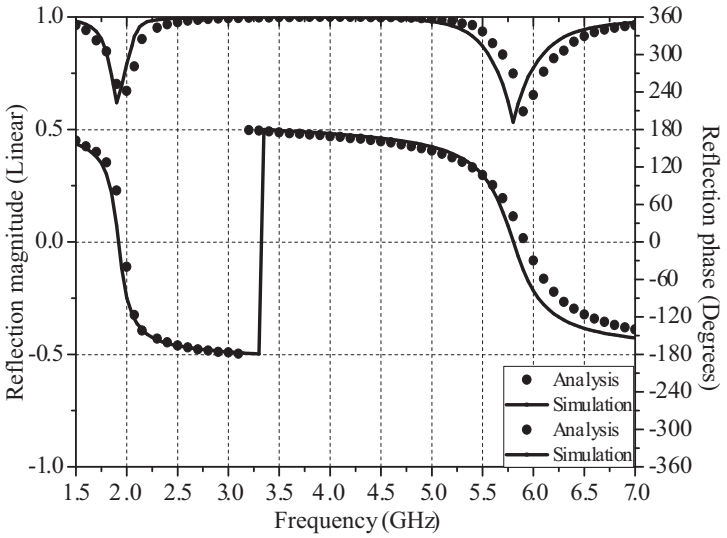

Figure 4. Analytic and simulated reflection coefficients of the proposed dual-band MTS.

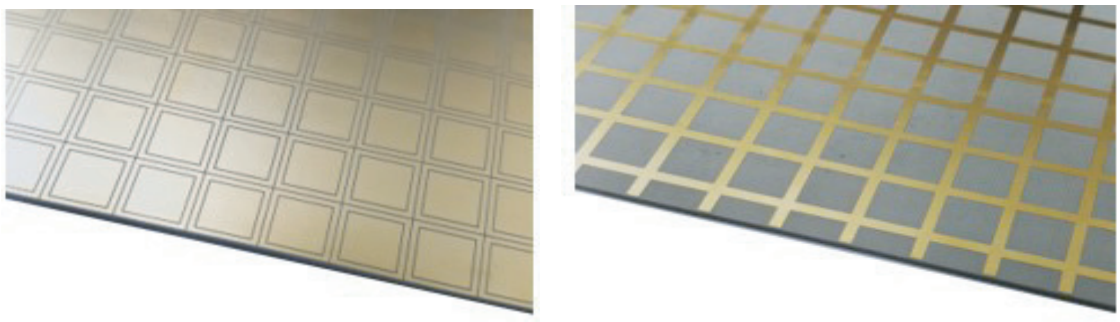

Figure 5. Photograph of the fabricated MTS (dimension = 144.5 mm × 144.5 mm, number of unit cell = 17 × 17). (a) One side. (b) The other side.

in Fig. 8. The lengths of the ring patch and rectangular patch (l_H) correspond approximately to one wavelength and half wavelength in the low and high bands, respectively. The gap coupled structure is employed to feed at two different radiators simultaneously, and the impedance matching of both antennas can be controlled by its length (l_F) and width (w_F). The design parameters of the patch antenna for 2.1 GHz and 5.8 GHz are as follows: $w_L = 19.5$ mm, $l_L = 12.2$ mm, $w_H = 15$ mm, $l_H = 7$ mm, $w_F = 7$ mm, $l_f = 0.5$ mm, $S = 144.5$ mm. Also, the utilized substrate has a thickness of 1.6 mm and relative permittivity of 10.2. The proposed dual-band superstrate antenna is fabricated as shown in Fig. 9. Fig. 10 shows the full-wave simulated and measured reflection coefficients of the proposed antenna with and without MTS. In the case of the dual-band superstrate antenna, the height of MTS is 12 mm as calculated in Section 2. The measured results are obtained using Agilent 8510C vector network analyzer (VNA). The measured resonant frequencies of dual-band superstrate antenna are 2.08 GHz and 5.82 GHz, and are also in agreement with the simulated results. The undesired resonance at 6.01 GHz from measured results arises from a slot mode between ring and patch, and its radiation pattern is omnidirectional.

The far-field radiation patterns are measured in an anechoic chamber system to confirm performance of the dual-band MTS. The anechoic chamber is composed of shield enclosure (Size 4 m × 2.5 m × 2.5 m), 18-inch pyramidal absorber, network analyzer, wireless communication test set, positioner, turn table, and a dual-polarized transmit antenna. The simulated and measured far-field radiation patterns at low

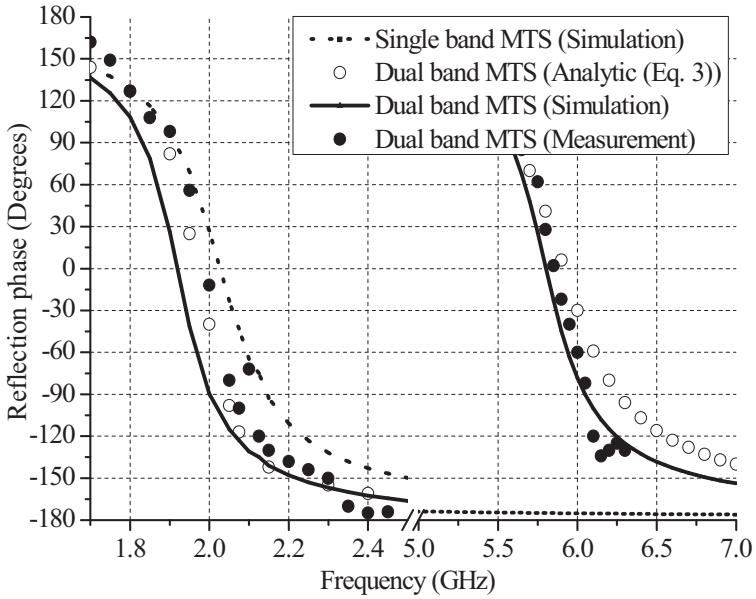

Figure 6. Analytic, full-wave simulated, and measured reflection phase of MTS (Single & dual band).

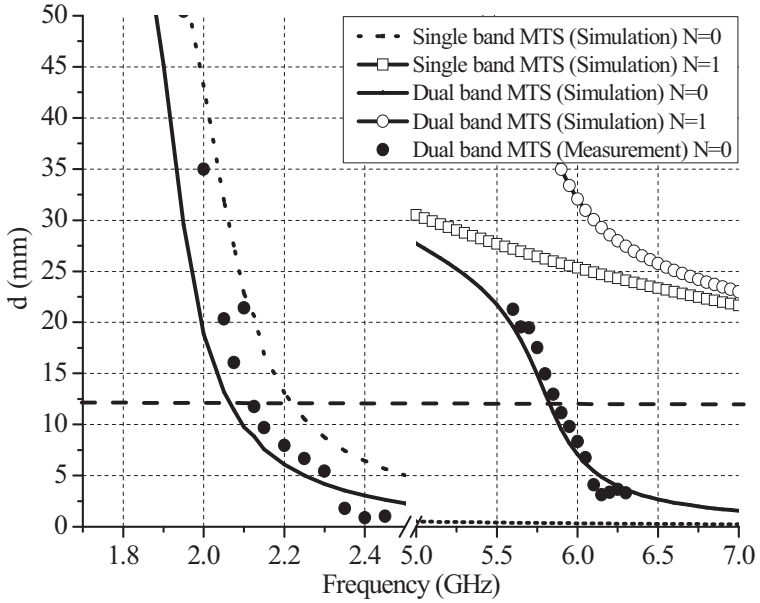

Figure 7. Comparison of height (d) satisfying resonance condition for single band and dual-band MTS.

and high bands are compared in Fig. 11 and Fig. 12, respectively. The gain improvement in the low and high bands are measured to be 4.1 dB and 3.2 dB, respectively. Also, the reflection magnitudes of the designed MTS at 2.08 GHz and 5.82 GHz are 0.61 and 0.53, respectively. From Equation (1), the estimated maximum gains at low and high bands can be improved as 6 dB and 4.5 dB in the infinite ground condition, respectively. Since the dimension of the designed superstrate antenna is about $1\lambda_0$ (at 2.08 GHz) and $3\lambda_0$ (at 5.82 GHz) and is not infinite, the maximum gain improvement cannot be obtained. Moreover, even though reflection magnitude of the PRS needs high value for a maximum gain improvement, we have focused on design of dual-band superstrate antenna in this paper. The simulated and measured results are in good agreement except for gain improvement of less than about 1 dB. The insufficient gain improvement seems caused by a connector loss and misalignment between the

source radiator and the MTS. Also, the measured gains of the planar patch antenna with and without MTS against frequencies are shown in Fig. 13. Applying the MTS in the patch antenna, the gain bandwidth is narrower than that of the patch antenna without MTS because the resonance condition

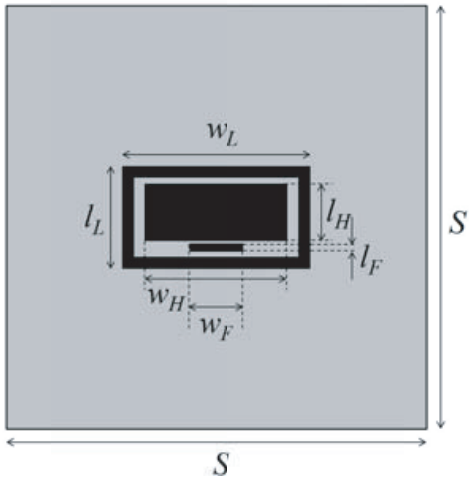

Figure 8. Structure of a dual-band planar patch antenna.

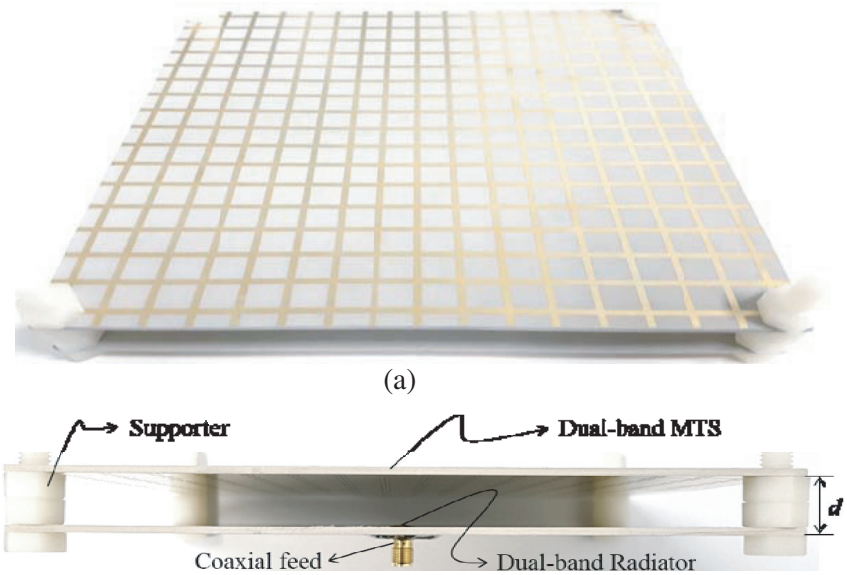

Figure 9. Photograph of the fabricated dual-band superstrate antenna. (a) Top view. (b) Side view.

Table 1. Compared characteristics of superstrate antennas.

	This work	**Ref. [1]**	**Ref. [6]**	**Ref. [7]**	**Ref. [8]**
d (Height of PRS)	$0.08\lambda_0/0.23\lambda_0$	$0.4375\lambda_0$	$0.25\lambda_0$	$0.0625\lambda_0$	$0.016\lambda_0$
Band	Dual-band	Single-band	Single-band	Single-band	Single-band
Via process	No	No	No	Yes	No
# of artificial surface	1		1	1	2

of a cavity should be satisfied. Basically, the gain bandwidth of a superstrate antenna depends on the phase slope of a PRS, and a broader gain bandwidth could be obtained after the optimization of an MTS. The overall performance of the proposed antenna is compared with the reported FPC antennas in Table 1. Even though the height of the proposed antenna is higher than those of Refs. [7] and [8], it has advantages such as dual-band operation, no via hole fabrication, and phase control of one artificial surface. The artificial surface means that the reflection phase of a certain surface can be changed from -180° to 180° using a metallic pattern to reduce height of the superstrate antenna. Since the proposed antenna in this paper is concentrated on operation in dual-band, it can be designed to have a much lower profile.

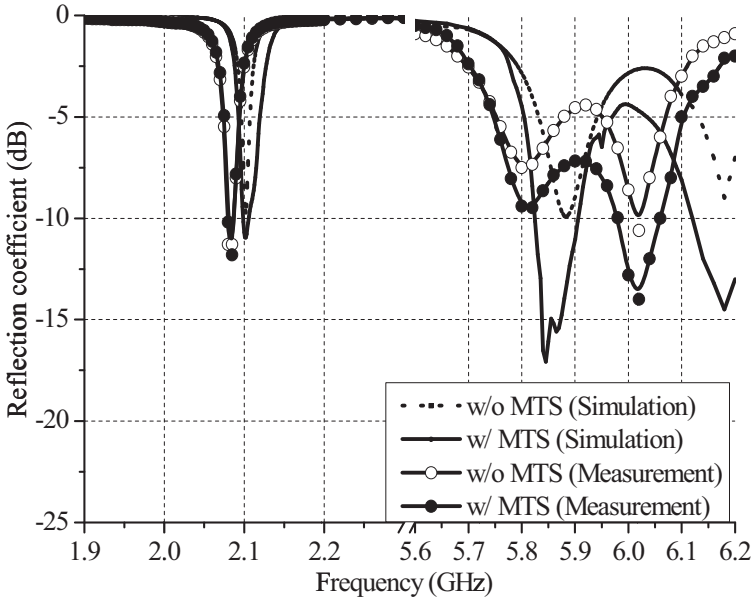

Figure 10. Full-wave simulated and measured reflection coefficient of planar patch antenna without and with MTS.

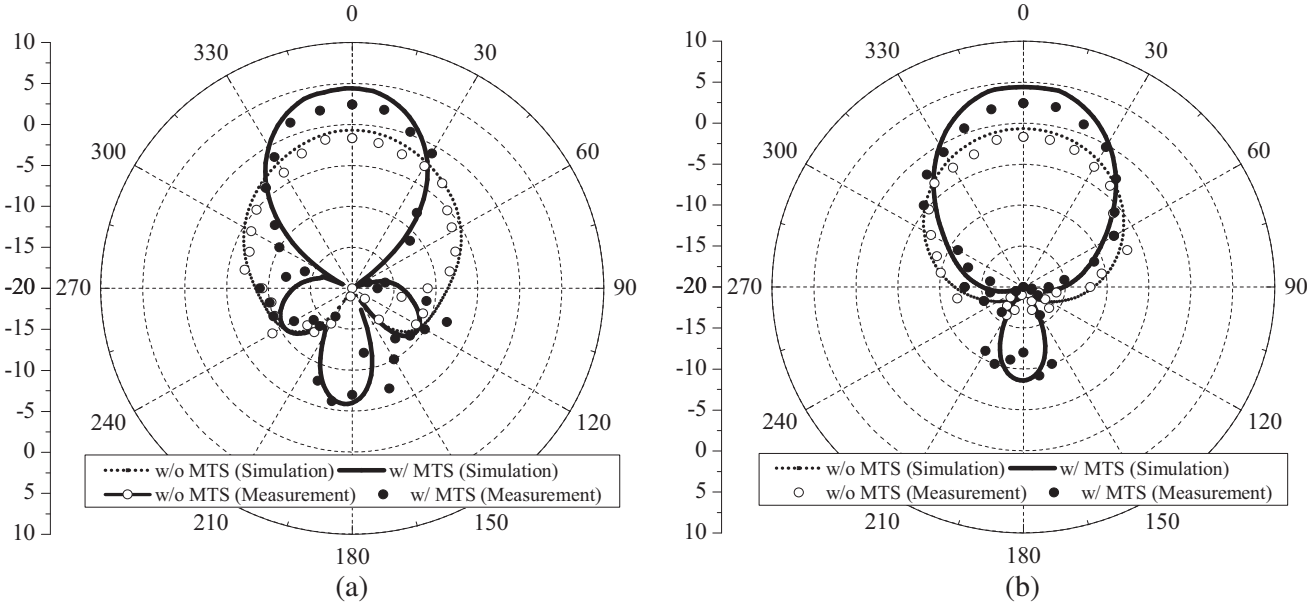

Figure 11. Simulated and measured far-field radiation patterns at low band. (a) E-plane. (b) H-plane.

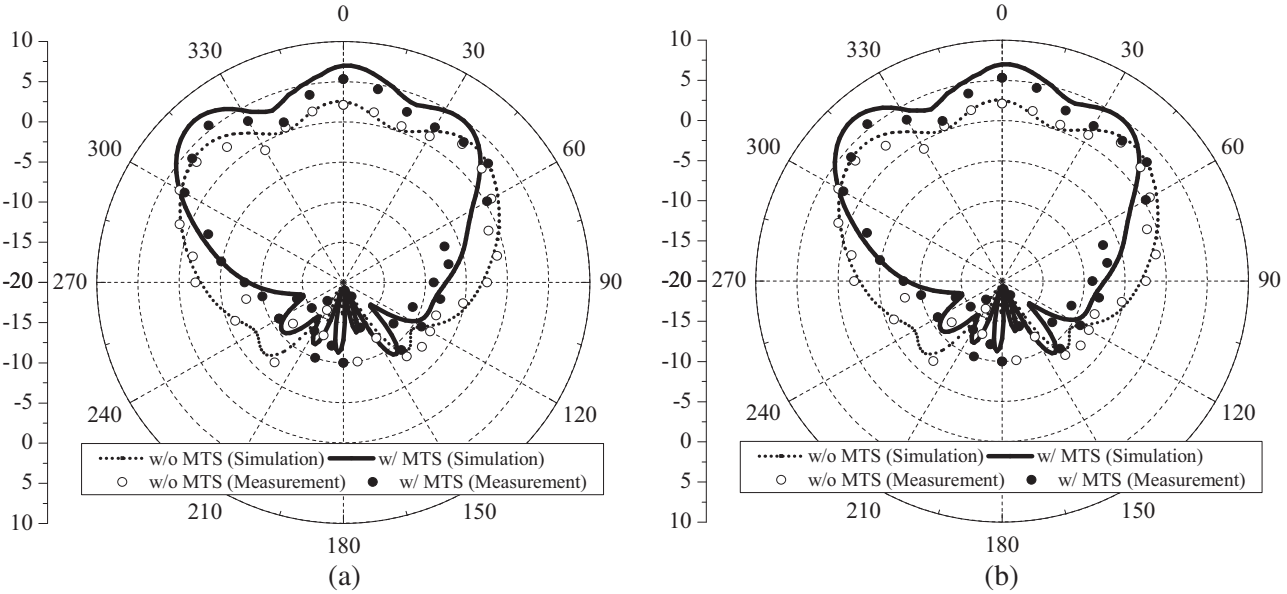

Figure 12. Simulated and measured far-field radiation patterns at high band. (a) E-plane. (b) H-plane.

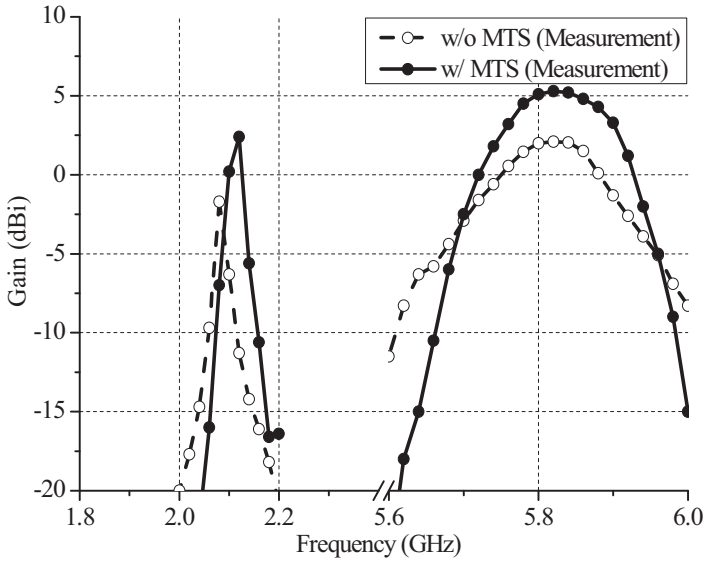

Figure 13. Measured gain of the planar patch antenna without and with MTS against frequencies.

4. CONCLUSION

In this paper, a low-profile dual-band superstrate antenna, which is operated as a FPC antenna, is proposed using a dual-band MTS. The employed MTS as a superstrate has a zero degree reflection phase at dual-band and is composed of a substrate, periodic metallic square patches and rings on the lower face, and periodic metallic meshes on the upper face. Also, the planar radiator is designed using a ring patch and a rectangular patch having a gap feed operated at 2.1 GHz and 5.8 GHz, respectively. A height of MTS from the ground plane is 12 mm. The height of 12 mm corresponds to about $0.08\lambda_0$ and $0.23\lambda_0$ at operation frequencies of radiator, respectively. The measured peak gains are increased by 4.1 dB and 3.2 dB at low and high bands, respectively.

ACKNOWLEDGMENT

This research was supported by Basic Science Research Program through the National Research Foundation of Korea (NRF) funded by the Ministry of Education (No. 2015R1A6A1A03031833) and MSIP (Ministry of Science, ICT and Future Planning), Korea, under the ITRC (Information Technology Research Center) support program (IITP-2017-2016-0-00291) supervised by the IITP (Institute for Information & communications Technology Promotion).

REFERENCES

1. Trentini, G. V., "Partially reflecting sheet arrays," *IRE Trans. on Antennas and Propagation*, Vol. 4, 666–671, Oct. 1956.
2. Jackson, D. R. and N. G. Alexopoulos, "Gain enhancement methods for printed circuit antennas," *IEEE Trans. on Antennas and Propagation*, Vol. 33, No. 9, 976–987, Sep. 1985.
3. Yang, H. Y. and N. G. Alexopoulos, "Gain enhancement methods for printed circuit antennas through multiple superstrates," *IEEE Trans. on Antennas and Propagation*, Vol. 35, No. 7, 860–863, Jul. 1987.
4. Sievenpiper, D., L. Zhang, R. F. J. Broas, N. G. Alexopoulos, and E. Yablonovitch, "High-impedance electromagnetic surfaces with a forbidden frequency band," *IEEE Trans. on Microwave Theory and Technique*, Vol. 47, No. 11, 2059–2074, Nov. 1999.
5. Holloway, C. L., M. A. Mohamed, E. F. Kuester, and A. Dienstfrey, "Reflection and transmission properties of a metafilm: With an application to a controllable surface composed of resonant particles," *IEEE Trans. on Electromagnetic Compatibility*, Vol. 47, No. 4, 853–865, Jan. 2005.
6. Feresidis, A. P., G. Goussetis, S. Wang, and J. C. Vardaxoglou, "Artificial magnetic conductor surfaces and their application to low-profile high-gain planar antennas," *IEEE Trans. on Antennas and Propagation*, Vol. 53, No. 1, 209–214, Jan. 2005.
7. Zhou, L., H. Li, Y. Qin, Z. Wei, and C. T. Chan, "Directive emissions from subwavelength metamaterial-based cavities," *Applied Physics Letters*, Vol. 86, 2005.
8. Ourir, A., A. Lustrac, and J. Lourtioz, "All-metamaterial-based subwavelength cavities for ultrathin directive antennas," *Applied Physics Letters*, Vol. 88, 2006.
9. Yahiaoui, R., S. N. Burokur, and A. de Lustrac, "Enhanced directivity of ultra-thin metamaterial-based cavity antenna fed by multisource," *Electronics Letters*, Vol. 45, No. 16, 814–816, 2009.